Revista Mexicana de Astronomía y Astrofísica, **47**, 75–82 (2011)

RECALIBRATED TURBULENCE PROFILES AT SAN PEDRO MÁRTIR

R. Avila,[1,2] L. J. Sánchez,[3] I. Cruz-González,[3] E. Carrasco,[4] and V. M. Castaño[5,6]

Received 2010 December 1; accepted 2011 January 21

RESUMEN

La calibración de perfiles de turbulencia óptica (C_N^2) medidos con el método SCIDAR generalizado ha sido recientemente revisada y corregida por Avila & Cuevas (2009). Basándonos en ese trabajo, aquí presentamos la corrección de todos los perfiles de C_N^2 medidos con el SCIDAR generalizado en el Observatorio Astronómico Nacional de San Pedro Mártir. El perfil de C_N^2 mediano corregido conserva su estructura vertical general. El cociente promediado en altura de la mediana de los valores de C_N^2 corregidos sobre la mediana de los valores no corregidos es igual a 0.87. La mediana del *seeing* corregido en el sitio es $0\farcs68 \pm 0\farcs03$, 4.2% menor que la mediana no corregida. Las medianas del *seeing* producido por turbulencia en los dos primeros kilómetros de altura sobre los telescopios de 1.5 m y 2.1 m de diámetro decrecen en un 15.8% y 13.6%, respectivamente. El ángulo isoplanático corregido tiene una mediana de $1\farcs96 \pm 0\farcs04$.

ABSTRACT

The calibration of optical turbulence (C_N^2) profiles measured with the generalized SCIDAR technique has been recently reviewed and corrected by Avila & Cuevas (2009). Based on that work, here we present the correction of all the C_N^2 profiles measured with a generalized SCIDAR at the Observatorio Astronómico Nacional of San Pedro Mártir. The median corrected C_N^2 profile conserves its overall vertical shape. The altitude-averaged ratio of the corrected median C_N^2 values over the uncorrected ones equals 0.87. The corrected median value of seeing at the site is $0\farcs68 \pm 0\farcs03$, 4.2% lower than the median value obtained with the uncorrected profiles. The median values of the seeing produced by turbulence in the first 2 km above the 1.5 m and the 2.1 m telescopes decrease by 15.8% and 13.6%, respectively. The corrected isoplanatic angle has a median value of $1\farcs96 \pm 0\farcs04$.

Key Words: atmospheric effects — instrumentation: high angular resolution — site testing

1. INTRODUCTION

Scintillation detection and ranging (SCIDAR) is an efficient technique to measure optical turbulence profiles, that is, the vertical distribution of the refractive-index structure constant, $C_N^2(h)$. The method is based on the determination of the normalized spatial autocovariance of the intensity distribution (scintillation) detected on the pupil plane of a telescope. The first version of this technique (Rocca, Roddier, & Vernin 1974) –known as Classical SCIDAR– was only sensitive to turbulence located higher than one kilometer above the ground, thus failing to detect turbulent layers near the ground, which are now known to be the most intense (Avila, Vernin, & Cuevas 1998; Egner, Masciadri, & McKenna 2007; Fuensalida et al. 2007; Chun et al. 2009; García-Lorenzo et al. 2009; Masciadri et al. 2010). Fuchs, Tallon, & Vernin (1994) proposed that turbulence near the ground would be measurable if instead of recording the scintillation on the telescope pupil plane, the detector was made the

[1]Centro de Física Aplicada y Tecnología Avanzada, Universidad Nacional Autónoma de México, Mexico.

[2]On leave from Centro de Radioastronomía y Astrofísica, Universidad Nacional Autónoma de México, Mexico.

[3]Instituto de Astronomía, Universidad Nacional Autónoma de México, Mexico.

[4]Instituto Nacional de Astrofísica Óptica y Electrónica, Mexico.

[5]Universidad Autónoma de Querétaro, Campus Cerro de las Campanas, Mexico.

[6]On sabatical leave from Centro de Física Aplicada y Tecnologá Avanzada, Universidad Nacional Autónoma de México, Mexico.

conjugate of a virtual plane located a few kilometers below the pupil (analysis plane). Avila, Vernin, & Masciadri (1997) put that idea in practice for the first time, showing its efficiency. This new configuration, called Generalized SCIDAR (GS), has been vastly used to characterize astronomical sites (Avila et al. 1997; Fuchs, Tallon, & Vernin 1998; Klückers et al. 1998; Avila et al. 1998; Kern et al. 2000; Avila, Vernin, & Sánchez 2001; Prieur, Daigne, & Avila 2001; Wilson et al. 2003; Avila et al. 2004; Tokovinin et al. 2005; García-Lorenzo & Fuensalida 2006; Egner et al. 2007; Vernin et al. 2007; Egner & Masciadri 2007; Avila et al. 2008; Fuensalida, García-Lorenzo, & Hoegemann 2008; García-Lorenzo & Fuensalida 2011; Masciadri et al. 2010). The method and the physics involved in either version of the SCIDAR technique have thoroughly been treated by a number of authors (Rocca et al. 1974; Vernin & Azouit 1983a,b; Klückers et al. 1998; Prieur et al. 2001).

Recently, Avila & Cuevas (2009) –inspired by Johnston et al. (2002)– demonstrated that the algebraic method customarily used in GS for the normalization of the scintillation autocovariance leads to overestimated C_N^2values, and proposed a procedure for the correct recalibration of the turbulence profiles. The relative error can take values from zero to a factor of 4, depending on the telescope size, the double star used as source, the position of the analysis plane and the turbulence altitude. Until now, turbulence profiles at Mt Graham (Masciadri et al. 2010) and El Teide (García-Lorenzo & Fuensalida 2011) observatories have been recalibrated using that procedure.

In 1997 and 2000, GS measurements were carried out at the Observatorio Astronómico Nacional de San Pedro Mártir (OAN-SPM), Baja California, Mexico. Avila et al. (2004, hereafter A04) report a statistical analysis of the $C_N^2(h)$ measured in both campaigns. Avila et al. (1998) present the results of the 1997 campaign and Avila et al. (2006) give a statistical analysis of wind speed profiles and wavefront coherence time. In view of the newly discovered calibration issue, a reanalysis of the GS results at the OAN-SPM is in order. Here we present the correction of the C_N^2 values and its implications on the statistical description of the seeing and isoplanatic angle. In § 2 the observation campaigns and original data are described. § 3 is devoted to the description of the C_N^2 values correction and the statistical analysis of the corrected turbulence profiles is presented in § 4. Finally the discussion and conclusions are given in § 5.

TABLE 1

TELESCOPES WHERE THE GS WAS INSTALLED

	Diameter (D)[a]	Secondary over Primary (e)
SPM2.1	2.1	0.27
SPM1.5	1.5	0.26

[a]In meters.

2. OBSERVATION CAMPAIGN AND DATA OVERVIEW

Two GS observation campaigns have been carried out at the OAN-SPM in 1997 and 2000, respectively. In 1997, the GS was installed at the 1.5 m and 2.1 m telescopes (SPM1.5 and SPM2.1) for 8 and 3 nights (1997 March 23–30 and April 20–22 UT), whereas in 2000 the instrument was installed for 9 and 7 nights (May 7–15 and 16–22 UT) at SPM1.5 and SPM2.1. It is fair to mention that in the 2000 campaign additional instruments (Masciadri, Avila, & Sánchez 2004) were deployed, even though they have no impact on the present article.

The numbers of $C_N^2(h)$ samples obtained in 1997 and 2000 were 3398 and 3016, respectively, making a total of 6414. The altitude scale of the profiles refers to altitude above sea level (2800 m at OAN-SPM). In GS data, part of the turbulence measured at the observatory altitude is produced inside the telescope dome. For site characterization, this contribution must be subtracted. In all the analyses presented here, dome turbulence has been removed using the procedure explained in A04. Almost all the time the most intense turbulence was located at the observatory altitude.

3. C_N^2VALUES CORRECTION

The GS technique is based on the estimation of the normalized spatial autocovariance $\mathcal{C}$ of a double-star scintillation recorded on a virtual plane located a distance d below the ground (of the order of a few kilometers). The procedure to estimate the scintillation autocovariance is to compute the mean autocorrelation of double-star scintillation images, normalized by the autocorrelation of the mean image. In the classical SCIDAR –where images are taken at the telescope pupil– this computation leads analytically to $\mathcal{C}$ (Rocca et al. 1974). However for the GS, Johnston et al. (2002) show that the result of this procedure is not equal to $\mathcal{C}$. The discrepancy is due to the shift of the out-of-focus pupil images pro-

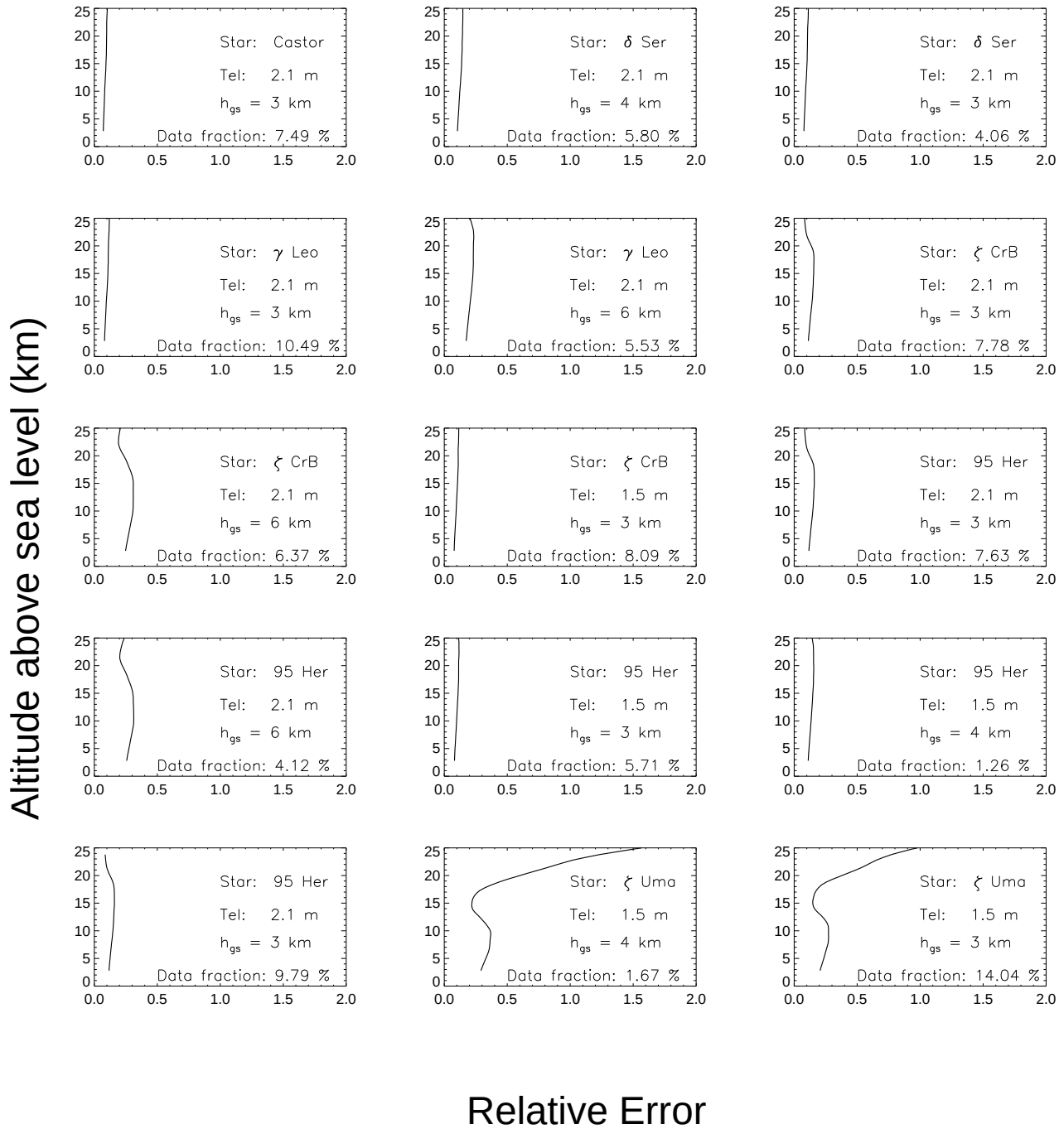

Fig. 1. Vertical profiles of the relative error. Each plot corresponds to a different combination of the parameters that define the relative error. Those parameters are indicated in each plot box together with the fraction of the data that was taken with the corresponding parameter set.

duced by each star on the detector. Those authors analyze this effect only for turbulence at ground level ($h = 0$). Avila & Cuevas (2009, hereafter AC09) generalize the analysis to turbulence at any height and provide an analytical formula for the calculation of the relative error ϵ induced on the C_N^2 values by the wrong normalization. AC09 provide exact and approximate –easier to compute– formulae for ϵ. In this paper, only the exact expression (equation 32 in AC09) is used. The general dependence of ϵ upon

TABLE 2

STELLAR SOURCES USED FOR GS MEASUREMENTS

Name	α_{2000}[a]	δ_{2000}[b]	Δm[c]	b[d]	θ[e]
Castor	7 34	31 53	2.1	0.19	4.0
γ Leo	10 20	19 50	1.3	0.16	4.5
ζ Uma	13 24	54 56	1.6	0.15	14.4
δ Ser	15 35	10 32	0.9	0.20	4.0
ζ Cbr	15 39	36 38	0.9	0.20	6.4
95 Her	18 01	21 36	0.4	0.25	6.3

[a]Right ascension in hours and minutes.

[b]Declination in degrees and arc minutes.

[c]Visible magnitude difference.

[d]See text and equation (24) in AC09.

[e]Angular separation in seconds of arc.

the observational parameters is as follows: the relative error is an increasing function of the turbulence altitude h, the double star separation θ, the conjugation distance d and the magnitude difference Δm of the double-star components. The relative error decreases as the telescope diameter D increases. The ratio e of the secondary over the primary mirror diameters has an influence on the shape of the plot ϵ vs. h, as can be seen in Figure 5 of AC09. For the sake of consistency with AC09, the magnitude difference of the stellar components is expressed through the parameter b defined by equation 24 in AC09. The values of D and e for the telescopes used in the OAN-SPM GS measurements are given in Table 1 and the stellar sources in Table 2.

The vertical profile of the relative error, $\epsilon(h)$, has been computed for the corresponding parameter values of the campaigns. The profiles are plotted in Figure 1. The percentage of data taken with each parameter set is indicated in the corresponding frame. The relative error is most of the time between 0.05 and 0.25 (5% to 25%). However, when ζ Uma is used (last two frames), ϵ reaches very high values at high altitude.

The correct $C_{\rm N}^2(h)$ are obtained by multiplying the original profiles by $1/(1+\epsilon(h))$. Each of the 6414 $C_{\rm N}^2$ profiles was so corrected.

The uncertainty of the statistical values given throughout the paper was estimated using the bootstrap method (Efron 1982), as explained in Appendix A of A04.

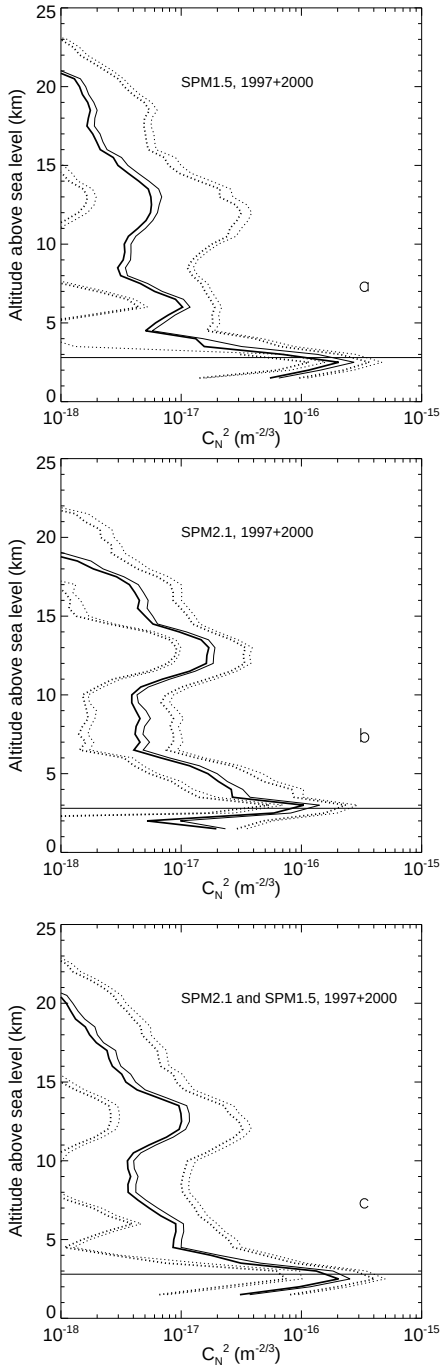

Fig. 2. Median (full line), 1st and 3rd quartiles (dashed lines) of the $C_{\rm N}^2(h)$ values obtained with the GS at the (a) 1.5mT, (b) 2.1mT and (c) both telescopes, during the 1997 and 2000 campaigns. Bold and thin lines correspond the corrected and non-corrected values, respectively. The horizontal axis represents $C_{\rm N}^2$ values, on a logarithmic scale, and the vertical axis represents the altitude above sea level. The horizontal lines indicate the observatory altitude. Dome seeing has been removed.

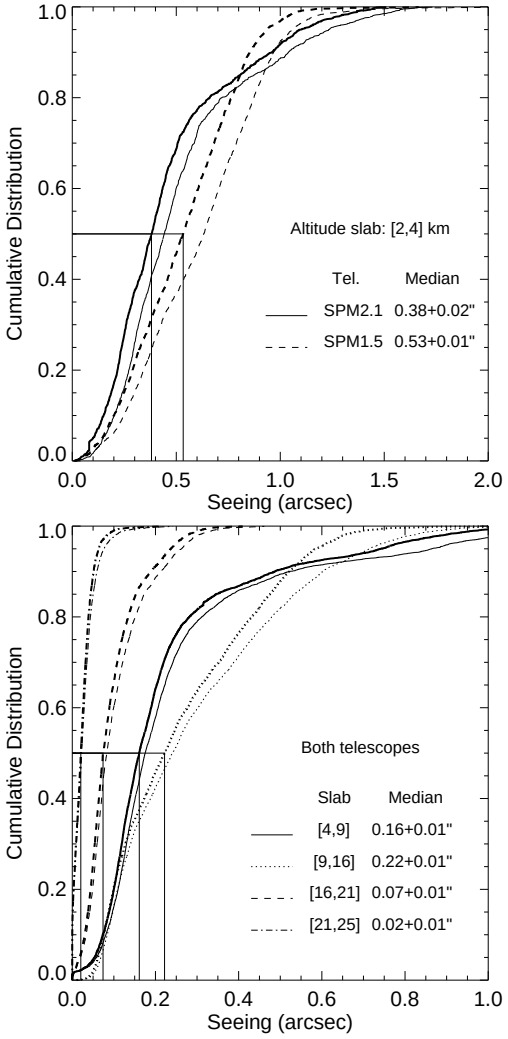

Fig. 3. Cumulative distributions of the seeing generated in different atmosphere slabs: (top)]2, 4] km for the 2.1mT (full line) and the 1.5mT (dashed line) without dome seeing; (bottom)]4, 9] km (full line),]9, 16] km (dotted line),]16, 21] km (dashed line),]21, 25] km (dash-dotted line). Data used: 1997 and 2000 campaigns. Bold and thin lines correspond the corrected and non-corrected values, respectively. Horizontal and vertical lines indicate corrected median values, which are reported in Table 3 together with the 1st and 3rd quartiles.

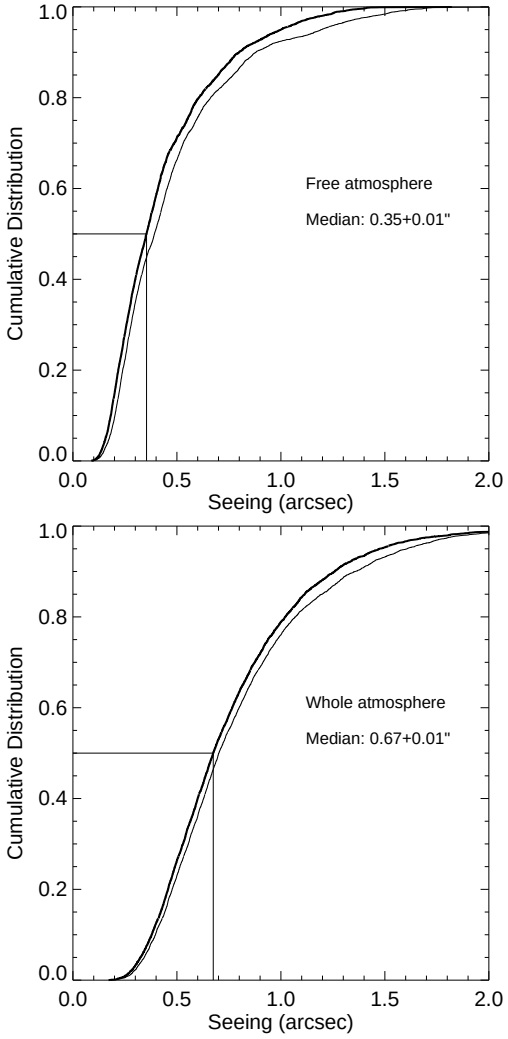

Fig. 4. Cumulative distributions of the seeing generated in (top) the free atmosphere (altitude higher than 4 km) and (bottom) the whole atmosphere, without dome seeing. Data from both telescopes and both campaigns are included.Bold and thin lines correspond the corrected and non-corrected values respectively. The horizontal and vertical lines indicate the corrected median values, which are reported in Table 3 together with the 1st and 3rd quartiles.

4. STATISTICAL ANALYSIS OF CORRECTED PROFILES

The median, first and third quartile profiles of the $C_N^2(h)$ data measured with SPM1.5 and SPM2.1 are shown in Figures 2a and 2b, respectively. In Figure 2c, the same kind of profiles are shown for the complete GS data set. It can be seen that the shape of those profiles is not altered by the correction. All the plots are basically only shifted towards lower values by a similar amount, which on a logarithmic scale corresponds to being multiplied by a factor. The average shift factor of all the quartile profiles shown in Figure 2 is 0.87.

As explained in A04, at ground level the turbulence at the 1.5 m telescope is more intense than that at the 2.1 m telescope, presumably because the later

TABLE 3

SEEING FOR DIFFERENT ATMOSPHERE SLABS AND VARIATION

Slab (km)	First Quartile (arcsec)	Median (arcsec)	Third Quartile (arcsec)
[2, 4] @ SPM2.1[a]	0.24[b] (−20.0%)	0.38[c] (−13.6%)	0.55[d] (−12.7%)
[2, 4] @ SPM1.5[a]	0.32[b] (−15.8%)	0.53[b] (−15.8%)	0.71[b] (−14.5%)
[4, 9]	0.11[b] (−8.3%)	0.16[b] (−5.9%)	0.24[b] (−11.1%)
[9, 16]	0.11[b] (−8.3%)	0.22[b] (−8.3%)	0.39[b] (−9.3%)
[16, 21]	0.04[b] (−20.0%)	0.07[b] (−12.5%)	0.12[b] (−14.3%)
[21, 25]	0.01[b] (0.0%)	0.02[b] (0.0%)	0.03[b] (−25.0%)
Free atmosphere: [4, 25]	0.24[b] (−7.7%)	0.35[b] (−10.2%)	0.55[b] (−6.8%)
Whole atmosphere.: [2, 25][e]	0.50[b] (−3.8%)	0.68[b] (-4.2%)	0.97[c] (−2.0%)

[a]Without dome seeing.

[b]Uncertainty: ±0.01.

[c]Uncertainty: ±0.02.

[d]Uncertainty: ±0.03.

[e]As if measured at the SPM2.1 and without dome seeing.

is on top of a 20 m high building whereas the former is at ground level. The general vertical structure of the turbulence distribution from the whole data set can be summarized as a strong layer at the ground, and two thick layers centered at 6 and 13 km. The mean relative difference of the corrected and uncorrected median C_N^2 values is 15.2%, 19.3% and 15.4% for the data obtained at SPM1.5, SPM2.1 and for the complete data set.

The cumulative distribution of the corrected and uncorrected measurements of seeing generated within different altitude slabs is shown in Figure 3. For the 2–4 km slab, which includes ground turbulence, the data obtained at SPM2.1 and SPM1.5 are separated into two different cumulative distributions as ground contributions are different for each telescope. Similar plots are exhibited in Figure 4 for the free (above 4 km) and the whole atmosphere. Differences between the corrected and uncorrected cumulative distributions seem to be basically driven by seeing values. The larger the seeing value, the larger the difference. This is an expected behavior, since corrected and uncorrected C_N^2 are proportional to each other. The corrected values of median, first and third quartile of the seeing generated in the different slabs are summarized in Table 3. The variation of the corrected relative to the uncorrected values (reported in Table 3 of A04) is given in parentheses. Note that the vertical distribution of those relative variations does not follow any of the individual altitude profiles of the relative error $\epsilon(h)$, shown in Figure 1. This is due to the fact that the statistical values reported in Table 3 were obtained from a combination of different functions $\epsilon(h)$.

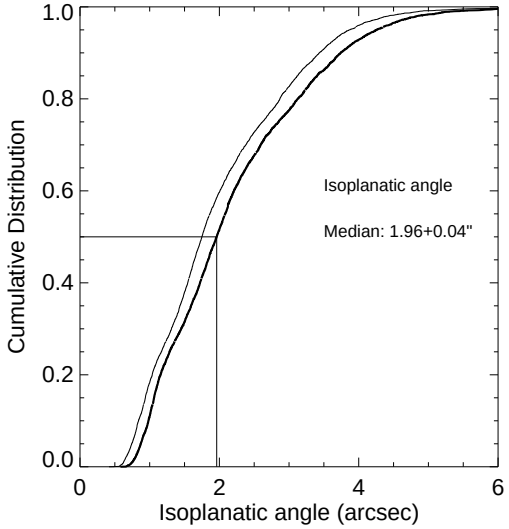

Fig. 5. Cumulative distribution of the isoplanatic angle θ_0 computed from each turbulence profile of both campaigns and both telescopes. Bold and thin lines correspond to the corrected and non-corrected values respectively. The corrected median value of θ_0 is $1\farcs96 \pm 0\farcs04$ and the 1st and 3rd quartiles are $1\farcs31 \pm 0\farcs04$ and $2\farcs86 \pm 0\farcs04$.

The isoplanatic angle θ_0 depends on C_N^2 and on its vertical distribution (see e.g. equations 5 and 6

from A04):

$$\theta_0 = \left[0.423 \left(\frac{2\pi}{\lambda}\right)^2 \int \mathrm{d}h\, h^{5/3} C_\mathrm{N}^2(h)\right]^{-3/5}, \quad (1)$$

where λ is the wavelength. Therefore, the correction of the C_N^2 profiles can have a strong impact on the values of θ_0. From each corrected $C_\mathrm{N}^2(h)$ one corrected value of the isoplanatic angle is obtained. The cumulative distribution of the corrected θ_0 is shown in Figure 5. The median value increased by the modest amount of 4.8% with respect to the median value of θ_0 obtained with the uncorrected turbulence profiles. However, under certain observation parameters and turbulence conditions, the isoplanatic angle increased significantly after the C_N^2 correction: in 10% of the cases, the increase was higher than 25%, and reached 40% in a few cases.

5. CONCLUSIONS

Although the impact on individual estimates of turbulence profiles caused by the correction of the normalization error may be very strong depending on the observational parameters – as deduced for example from the bottom right plot in Figure 1, the statistical parameters that describe the optical turbulence profiles measured at the OAN-SPM vary by a relatively small amounts after the correction. The vertical distribution of the median C_N^2 (on a logarithmic scale) remains basically the same as before the correction, the values being only multiplied by an average factor of 0.87. After correction, the median whole-atmosphere and free-atmosphere seeing diminished by 4.2% and 10.2% respectively, the correct values being 0.68 and 0.35 arc seconds. The altitude slab where the correction has the strongest impact is from 2 to 4 km, with a decrease in median seeing of 15.8% and 13.6% for measurements at SPM1.5 and SPM2.1. The corrected median value of the isoplanatic angle is $1\farcs96$ which represents an increase of 4.8% relative to the uncorrected value.

We are grateful to the OAN-SPM staff for their valuable support during the observation campaigns. This work was financially supported by Conacyt and PAPIIT through grants number 58291 and IN107109.

REFERENCES

Avila, R., Avilés, J. L., Wilson, R. W., Chun, M., Butterley, T., & Carrasco, E. 2008, MNRAS, 387, 1511
Avila, R., Carrasco, E., Ibáñez, F., Vernin, J., Prieur, J., & Cruz, D. 2006, PASP, 118, 503
Avila, R., & Cuevas, S. 2009, Optics Express, 17, 10926 (AC09)
Avila, R., Masciadri, E., Vernin, J., & Sánchez, L. 2004, PASP, 116, 682 (A04)
Avila, R., Vernin, J., & Cuevas, S. 1998, PASP, 110, 1106
Avila, R., Vernin, J., & Masciadri, E. 1997, Appl. Opt., 36, 7898
Avila, R., Vernin, J., & Sánchez, L. J. 2001, A&A, 369, 364
Chun, M., Wilson, R., Avila, R., Butterley, T., Aviles, J.-L., Wier, D., & Benigni, S. 2009, MNRAS, 394, 1121
Efron, B. 1982, The Jackknife, the Bootstrap and Other Resampling Plans (Philadelphia: The Society for Industrial and Applied Mathematics)
Egner, S. E., & Masciadri, E. 2007, PASP, 119, 1441
Egner, S. E., Masciadri, E., & McKenna, D. 2007, PASP, 119, 669
Fuchs, A., Tallon, M., & Vernin, J. 1994, Proc. SPIE, 2222, 682
_____. 1998, PASP, 110, 86
Fuensalida, J. J., García-Lorenzo, B., Delgado, J. M., Rodríguez-Hernández, M. A. C., & Vernin, J. 2007, RevMexAA (SC), 31, 86
Fuensalida, J. J., García-Lorenzo, B., & Hoegemann, C. 2008, MNRAS, 389, 731
García-Lorenzo, B., Eff-Darwich, A., Fuensalida, J. J., & Castro-Almazán, J. 2009, MNRAS, 397, 1633
García-Lorenzo, B., & Fuensalida, J. J. 2006, MNRAS, 372, 1483
_____. 2011, MNRAS, 410, 934
Johnston, R. A., Dainty, C., Wooder, N. J., & Lane, R. G. 2002, Appl. Opt., 41, 6768
Kern, B., Laurence, T. A., Martin, C., & Dimotakis, P. E. 2000, Appl. Opt., 39, 4879
Klückers, V. A., Wooder, N. J., Nicholls, T. W., Adcock, M. J., Munro, I., & Dainty, J. C. 1998, A&AS, 130, 141
Masciadri, E., Avila, R., & Sánchez, L. J. 2004, RevMexAA, 40, 3
Masciadri, E., Stoesz, J., Hagelin, S., & Lascaux, F. 2010, MNRAS, 404, 144
Prieur, J.-L., Daigne, G., & Avila, R. 2001, A&A, 371, 366
Rocca, A., Roddier, F., & Vernin, J. 1974, J. Opt. Soc. Am., 64, 1000
Tokovinin, A., Vernin, J., Ziad, A., & Chun, M. 2005, PASP, 117, 395
Vernin, J., & Azouit, M. 1983a, J. Optics (Paris), 14, 5
_____. 1983b, J. Optics (Paris), 14, 131
Vernin, J., Trinquet, H., Jumper, G., Murphy, E., & Ratkowski, A. 2007, Environmental Fluid Mech., 7, 371
Wilson, R. W., Wooder, N. J., Rigal, F., & Dainty, J. C. 2003, MNRAS, 339, 491

Remy Avila: Centro de Física Aplicada y Tecnología Avanzada, Universidad Nacional Autónoma de México, Apdo. Postal 1-1010, 76000 Santiago de Querétaro, Querétaro, México (r.avila@crya.unam.mx).
Esperanza Carrasco: Instituto Nacional de Astrofísica, Óptica y Electrónica, Luis Enrique Erro 1, 72840 Tonantzintla, Puebla, Mexico (bec@inaoep.mx).
Víctor M. Castaño: Universidad Autónoma de Querétaro, Campus Cerro de las Campanas, 76010 Querétaro, Querétaro, Mexico (castano@fata.unam.mx).
Irene Cruz-González and Leonardo J. Sánchez: Instituto de Astronomía, Universidad Nacional Autónoma de México, Apdo. Postal 70-264, 04510, México, D. F. Mexico (irene,leonardo@astroscu.unam.mx).